Proceeding Series of the Brazilian Society of Applied and Computational Mathematics, v. 6, n. 1, 2018.

Trabalho apresentado no XXXVII CNMAC, S.J. dos Campos - SP, 2017.

Proceeding Series of the Brazilian Society of Computational and Applied Mathematics

An efficient method for the numerical solution of blood flow in 3D bifurcated regions.

Luis Alonso Mansilla Alvarez[1]
Pablo Javier Blanco[2]
Raúl Antonino Feijóo[3]
National Laboratory for Scientific Computing, LNCC/MCTIC
National Institute of Science and Technology in Medicine Assisted by Scientific Computing, INCT-MACC

Abstract. From the point of view of the potential clinical use of computational hemodynamic, it is mandatory to get the computational time of simulation each time closer to real clinical needs. Spending hours and even days to solve accurately one single cardiac cycle of the whole cardiovascular system is unfeasible on daily practice. In this sense, in this work we study the transversally enriched pipe element method (TEPEM) as an effective alternative to solve the Navier-Stokes equations in bifurcated domains with enough accuracy to provide clinically relevant information but at a significantly reduced time.

Keywords. Hemodynamics, TEPEM, model order reduction, finite element method.

1 Introduction

The role of computational hemodynamics is fundamental to aid in the prognosis and diagnosis of cardiovascular diseases due the well-known correlation between the localization of these pathologies and hemodynamic quantities such as blood flow velocity, pressure, boundary layer separation and wall shear stress [4, 6, 7, 11]. Among many types of approaches available in the field of computational hemodynamics and considering the potential clinical use of these models, the trade-off between quality of results and computational burden is a key aspect. While fully 3D simulations are invaluable to our understanding of hemodynamics quantities and patterns, as recirculation within regions as aneurysms or stenoses, the high computational requirements of time and supercomputing clusters make this a difficult approach for common use in daily medical practice. Grinberg et al. report in [8] that simulating one cardiac cycle in an arterial tree that included the largest arteries required 27.7 hours of computational time using 40,000 processors. On the search of computationally cheaper approaches, dimensionally reduced models (e.g. 1D models) appear to be capable to provide useful information about the global dynamics

[1]lalvarez@lncc.br
[2]pjblanco@lncc.br
[3]feij@lncc.br

of the system with an excellent compromise between predictive capabilities and computational cost [1, 3, 5, 9, 12]. However, these reduced models are unable to predict some important features of cardiovascular function, such as local flow patterns and transversal dynamics. Considering this need for 3D-like results and looking for reduced computational effort (time and computational resources), it was proposed in [2, 10] the so-called transversally enriched pipe element method (TEPEM) as an effective numerical approach, capable to provide flow-related quantities with the sufficient accuracy to viabilize clinical use and with a severe reduction of the computational cost when compared with classical 3D simulation technologies. In this work, as a follow up study, we explore the advantages of the TEPEM for the simulation of blood flow through bifurcated domains in terms of time/resources reduction when compared with classical FEM approach.

2 Model problem

Let $\Omega \in \mathbb{R}^3$ with boundary $\Gamma = \Gamma_i \cup \Gamma_o \cup \Gamma_L$, being Γ_i and Γ_o the inlet and outlet boundaries, respectively. Lateral wall is smooth and is denoted by Γ_L. Figure 1 presents a diagram of the domain of analysis for the fluid flow problem.

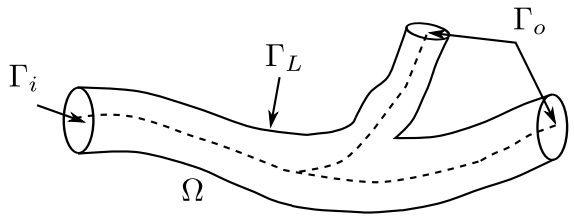

Figure 1: Schematic setting for the model problem

At Γ_i and Γ_o Neumann or Dirichlet boundary conditions can be imposed. Since we are modeling blood flow in an isolated geometry from the rest of the cardiovascular system, we assume the velocity field is fully developed at Γ_i and Γ_o, and thus homogeneous Dirichlet boundary conditions are considered for the in-plane velocity components. Additionally, Neumann boundary conditions are assumed for the normal component of the traction vector at those boundaries. Over Γ_L homogeneous Dirichlet boundary conditions are prescribed.

The variational formulation for the fluid flow problem reads: find $(\mathbf{u}, p) \in \boldsymbol{\mathcal{V}} \times L^2(\Omega)$ such that

$$\int_\Omega \left[\rho \frac{\partial \mathbf{u}}{\partial t} \cdot \hat{\mathbf{u}} + \rho(\nabla \mathbf{u})\mathbf{u} \cdot \hat{\mathbf{u}} + 2\mu \boldsymbol{\varepsilon}(\mathbf{u}) \cdot \boldsymbol{\varepsilon}(\hat{\mathbf{u}}) - p \operatorname{div} \hat{\mathbf{u}} - \hat{p} \operatorname{div} \mathbf{u} \right] d\Omega = \int_{\Gamma_i} t_i \mathbf{n} \cdot \hat{\mathbf{u}} \, d\Gamma_i + \int_{\Gamma_o} t_o \mathbf{n} \cdot \hat{\mathbf{u}} \, d\Gamma_o \qquad \forall (\hat{\mathbf{u}}, \hat{p}) \in \boldsymbol{\mathcal{V}} \times L^2(\Omega), \quad (1)$$

with ρ and μ being the fluid density and viscosity, respectively, $\boldsymbol{\varepsilon}(\cdot) = (\nabla(\cdot))^S$, $\mathbf{n}$ is the outward normal unit vector and $\hat{(\cdot)}$ denotes an admissible variation of field $(\cdot)$. Space $\boldsymbol{\mathcal{V}}$ is

$$\boldsymbol{\mathcal{V}} = \{\mathbf{u} \in \mathbf{H}^1(\Omega); \mathbf{u}|_{\Gamma_L} = 0, \, (\boldsymbol{\Pi}\mathbf{u})|_{\Gamma_i} = 0, \, (\boldsymbol{\Pi}\mathbf{u})|_{\Gamma_o} = 0\}, \quad (2)$$

DOI: 10.5540/03.2018.006.01.0312

where $\mathbf{H}^1(\Omega) = [H^1(\Omega)]^3$, and where $\mathbf{\Pi} = \mathbf{I} - \mathbf{n} \otimes \mathbf{n}$ is the projection operator over the surface whose normal unit vector is $\mathbf{n}$. Finally, t_i and t_o are given data which stand for the magnitude of the normal component of the traction vector imposed at Γ_i and Γ_o, respectively.

3 The TEPEM methodology

The TEPEM approach is based on the split of the axial and the transversal components of the primal fields on the Navier-Stokes equation: velocity and pressure. The motivation behind this strategy is the *a priori* knowledge on the blood flow dynamic, which features a dominant direction when circulating through the arterial system. To do this, we perform a very special partitioning strategy associated to an also unusual interpolant choice for the fields. These two steps are explained next.

3.1 Geometric approximation

As can be seen in [2, 10], the TEPEM associated partitioning is based on slab-type elements oriented following the axial direction of the domain. Then dealing with bifurcated domains, we must extend the partitioning strategy due the absence of one only dominant direction in the bifurcation region. In Figure 2 we show a first approach of slab-type partition of a bifurcated domain in which is easy to identify two types of elements: the *simple element* axially demarcated by two transversal sections and the *special element* axially demarcated by three transversal sections (colored in red).

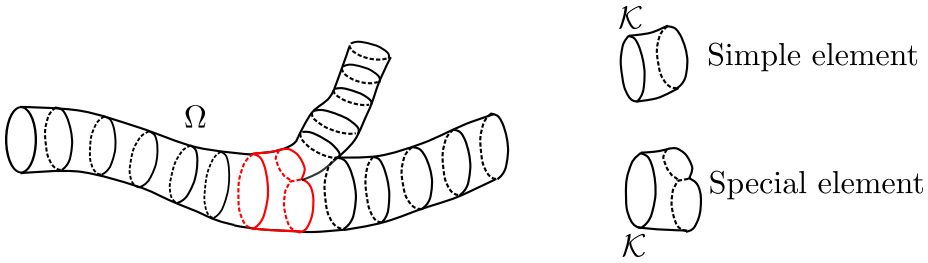

Figure 2: Geometrical partition of bifurcated domain based on slab-type elements.

Each element $\mathcal{K}$ is related to a reference element $\mathcal{K}_0$, here $\mathcal{K}_0 = [-1, 1]^3$, on the $\xi\eta\zeta-$space. Let us consider $\{S_i(\xi, \eta) : i = 1, \cdots, 12\}$ the cubic Serendipity family defined on the square $[-1, 1]^2$ of the $\xi\eta-$plane (see [10, 13]). The geometrical mapping between a slab-type element (simple or special) is based on a combination of Serendipity bases for each transversal section coupled with a quadratic approach for the axial direction.

A simple element $\mathcal{K}$ is composed by three transversal sections, two axial (flat) boundaries and one inner slice. Denoting by $\mathcal{S}_i (i = 1, 2, 3)$ the mapping between $[-1, 1]^2$ and each transversal section (via Serendipity basis), the map between the reference element and $\mathcal{K}$ is expressed as:

$$\chi_{\mathcal{K}}(\xi, \eta, \zeta) = \mathcal{S}_1(\xi, \eta)Q_1(\zeta) + \mathcal{S}_2(\xi, \eta)Q_2(\zeta) + \mathcal{S}_3(\xi, \eta)Q_3(\zeta) \tag{3}$$

On the other hand, a special element $\mathcal{K}$ is composed by four transversal sections, three axial (flat) boundaries and one inner slice. In a similar way to simple elements, denoting by $\mathcal{S}_i (i = 1, 2, 3, 4)$ the mapping between $[-1, 1]^2$ and each transversal section, the map between the reference element and $\mathcal{K}$ is expressed as:

$$\chi_{\mathcal{K}}(\xi, \eta, \zeta) = \mathcal{S}_1(\xi, \eta)Q_1(\zeta) + \mathcal{S}_2(\xi, \eta)Q_2(\zeta) + (\mathcal{S}_3(\xi, 2\eta - 1)\mathcal{I}_{\eta \geq 0} + \mathcal{S}_4(\xi, 2\eta + 1)\mathcal{I}_{\eta < 0})Q_3(\zeta) \tag{4}$$

With this interpolation basis and based only on the cross-section information, the geometrical mapping provides an accurate description of the real geometry, as can be seen in Figure 3. Notice that the geometrical approach, in the way explained here, is independent of the interpolant choice for the physical fields.

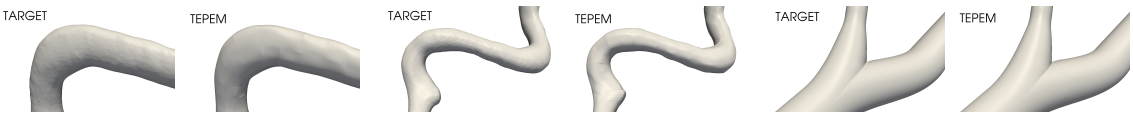

Figure 3: Comparison between three surface targets and the proposed geometry approach.

3.2 Physical fields approximation

Each field (in the reference element $\mathcal{K}_0$), is interpolated using a combination of low order polynomials in the axial direction and high order polynomials for the transversal (in-plane) direction. The order of the transversal interpolants will define the model capacity to deal with the transversal dynamics, the higher the order of the polynomial order for the transversal approach, the better the TEPEM solution. Denoting by p (p even) the transversal order, on the reference element $\mathcal{K}_0$ we approximate the velocity and pressure as:

$$u_h(\xi, \eta, \zeta) = \sum_{i=1}^{3} \sum_{j=1}^{(\mathsf{p}+1)^2} u_{ij}\phi_j(\xi, \eta)Q_i(\zeta) \qquad p_h(\xi, \eta, \zeta) = \sum_{i=1}^{2} \sum_{j=1}^{(\mathsf{p}/2+1)^2} p_{ij}\varphi_j(\xi, \eta)L_i(\zeta) \tag{5}$$

where $\{\phi_j\}$, $\{\varphi_j\}$, $\{Q_i\}$ and $\{L_i\}$ are basis functions of the spaces $\mathbb{P}_{\mathsf{p}} \times \mathbb{P}_{\mathsf{p}}$, $\mathbb{P}_{\mathsf{p}/2} \times \mathbb{P}_{\mathsf{p}/2}$, $\mathbb{P}_2$ and $\mathbb{P}_1$, respectively, with $\mathbb{P}_r$ the space of all the polynomials defined on $[-1, 1]$ with degree up to r. The reason behind this particular choice of spaces is to deal with the inf-sup condition. Even when the degrees of freedom per element is higher when compared against classical finite elements, the total number of unknowns in the system is considerable small due to the small quantity of slab-type elements.

4 Numerical results

To demonstrate the capacity of TEPEM, we simulate the flow through an idealized bifurcation. The boundary condition at the inlet is given by a prescribed flow such that the Reynolds number is Re = 250. At the outlet, homogeneous Neumann boundary condition is imposed. Fluid density and viscosity are set to $\rho = 1.04$ g/cm^3 and $\mu =$

0.04P, respectively. Due to the size of the problem, a distributed computing paradigm is employed for both, TEPEM and FEM approaches. Table 1 shows the results in terms of computational effort and accuracy for both methodologies and different mesh sizes for FEM and transversal order for the TEPEM. To measure the accuracy, we employed as reference solution a FEM approximation obtained with a very fine mesh composed by 4 903 064 degrees of freedom and 5 631 877 tetrahedral elements.

Table 1: Comparison of computational effort and acuracy for the TEPEM and FEM. All the cases for TEPEM and FEM are simulated using the same number of computational nodes.

		Computational effort			Error	
Method		Elements	DoFs	Time (min)	$\|v - v_h\|^2$	$\|p - p_h\|^2$
TEPEM	$\mathsf{p} = 4$	220	34 360	0.3	0.074243	116.27901
	$\mathsf{p} = 6$	220	68 266	2.4	0.029104	44.813802
	$\mathsf{p} = 8$	220	113 718	10.5	0.005007	25.730026
	$\mathsf{p} = 10$	220	170 716	36.1	0.003179	12.055404
	$\mathsf{p} = 12$	220	239 260	114.2	0.002485	6.2524727
FEM	$h = 0.012$	198 348	137 844	3.5	0.104832	112.57084
	$h = 0.01$	344 690	235 480	9.8	0.046576	60.573951
	$h = 0.008$	676 435	454 336	36.2	0.016205	26.188051
	$h = 0.006$	1 626 317	1 072 612	148.4	0.003197	9.8464527

The results in Table 1 illustrate the effectiveness of presented methodology on the reduction of computational effort and, at the same time, in the accuracy of results. The TEPEM, even with low transversal order such as $\mathsf{p} = 6$ or $\mathsf{p} = 8$, provides very reliable results capable to be employed for the computation of quantities of clinical interest, such as wall shear stress or fractional flow reserve, in a reasonable time. Figures 4 and 5, present a comparison between velocity field and pressure approximation using different approximation order of the TEPEM ($\mathsf{p} \in \{6, 8, 10\}$) against the refernce solution obtained using FEM. The velocity and pressure profiles provided by the TEPEM are very close to the reference solution using the FEM and, as expected, the higher the order of the polynomial order for the transversal approach, the better the TEPEM solution.

5 Final remarks

The strategy presented here is both simple and effective to provide sufficiently accurate with an important reduction in the computational effort. This method has now been extended to bifurcated domains. Hence, the TEPEM is seems promising targeting real applications in arterial patient-specific domains, because of its capacity to approximate flow-related quantities with precision compatible with medical demands.

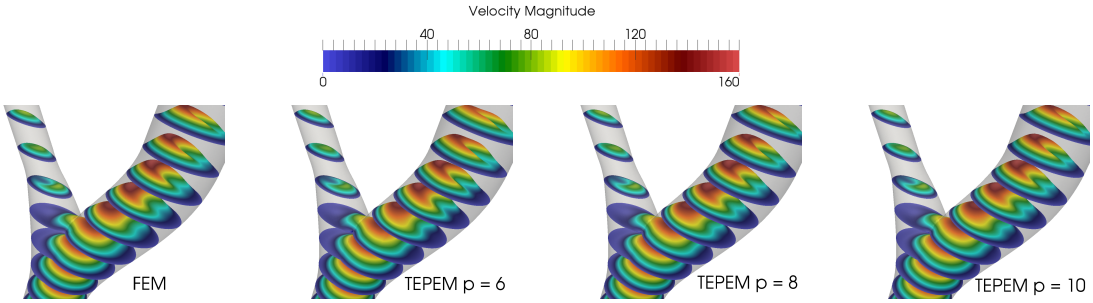

Figure 4: Comparison between the velocity magnitude of reference FEM solution and TEPEM approximations with different transversal enrichment.

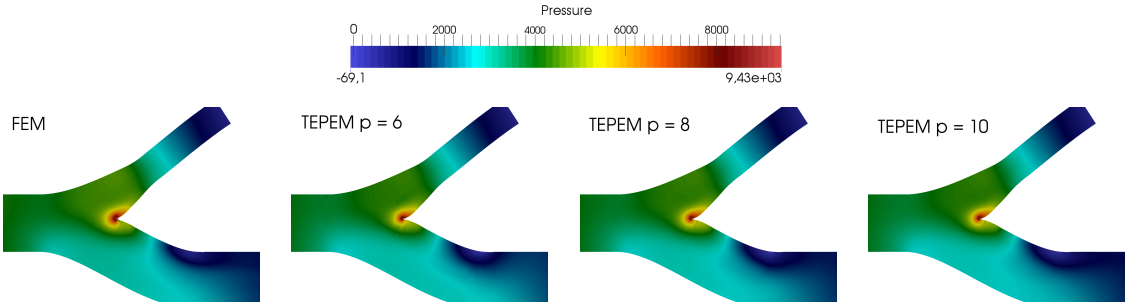

Figure 5: Comparison between the pressure profile of the reference FEM solution and TEPEM approximations with different transversal enrichment.

Acknowledgments

This work was partially suported by the Brazilian agencies CNPq and FAPERJ. The support of these agencies is gratefully acknowledged.

References

[1] A. P. Avolio. Multi-branched model of the human arterial system. *Med Biol. Engrg. Comp.*, 18:709–718, 1980.

[2] P. J. Blanco, L. A. Mansilla Alvarez and R. A. Feijóo. Hybrid element-based approximation for the Navier-Stokes equations in pipe-like domains. *Computer Methods in Applied Mechanics and Engineering*. 283:971–993, 2015.

[3] P. J. Blanco, S. M. Watanabe, E. A. Dari, M. A. R. Passos and R. A. Feijóo. Blood flow distribution in an anatomically detailed arterial network model: criteria and algorithms. *Biomechanics and modeling in mechanobiology*, 13(6): 1303–1330, 2014.

[4] A. Ü Coşkun, C. Chen, P. H. Stone and C. L. Feldman. Computational fluid dynamics tools can be used to predict the progression of coronary artery disease. *Physica A: Statistical Mechanics and its Applications*, 362(1): 182–190, 2006.

[5] L. Formaggia, D. Lamponi and A. Quarteroni. One-dimensional models for blood flow in arteries. *Journal of Engineering Mathematics*, 47:251–276, 2003.

[6] J. A. Fox and A. E. Hugh. Localization of atheroma: a theory based on boundary layer separation. *British Heart Journal*, 28(3): 388, 1996.

[7] G. D. Giannoglou, J. V. Soulis, T. M. Farmakis, D. M. Farmakis and G. E. Louridas. Haemodynamic factors and the important role of local low static pressure in coronary wall thickening. *International journal of Cardiology*, 86(1): 27–40, 2002.

[8] L. Grinberg, T. Anor, J. R. Madsen, A. Yakhot and G. E. Karniadakis. Large-scale simulation of the human arterial tree. *Clinical and Experimental Pharmacology and Physiology*, 36(2): 194–205, 2009.

[9] T. R. J. Hughes. On the one-dimensional theory of blood flow in the larger vessels. *Math. Biosciences*, 18:161–170, 1973.

[10] L. Mansilla Alvarez, P. Blanco, C. Bulant, E. Dari, A. Veneziani and R. Feijóo. Transversally enriched pipe element method (TEPEM): An effective numerical approach for blood flow modeling. *International Journal for Numerical Methods in Biomedical Engineering*, 2016. DOI: 10.1002/cnm.2808.

[11] U. Morbiducci, R. Ponzini, M. Grigioni and A. Redaelli. Helical flow as fluid dynamic signature for atherogenesis risk in aortocoronary bypass. A numerical study. *Journal of biomechanics*, 40(3): 519–534, 2007.

[12] N. Stergiopulos, D. F. Young and T. R. Rogge. Computer simulation of arterial flow with applications to arterial and aortic stenoses. *Journal of biomechanics*, 25(12):1477–1488, 1992.

[13] O. C. Zienkiewicz and R. L. Taylor. *The finite element method*. McGraw-hill, London, 1977.

